Magnetic resonance imaging differentiates locoregional flaps from free flaps after reconstructive surgical treatment of tongue cancer

Qijun Xu, MD,[a] Yu Lin, MD,[b] Zhen Xing, MD,[a] Tanhui Chen, MD,[a] Yingyan Zheng, MD,[a] and Dairong Cao, MD[a]

Objective. The aim of this study was to compare magnetic resonance imaging (MRI) features of reconstruction with locoregional flaps (LRFs) with free flaps (FFs) after surgical treatment for tongue cancer.

Study Design. In total, 115 cases of postoperative tongue carcinoma (67 cases of LRF surgery and 48 cases of FF surgery) were retrospectively reviewed. All patients had undergone nonenhanced and contrast-enhanced MRI at 0−4, 5−12, and 13−48 months after surgery. Signal intensity, margins, maximal size, contrast enhancement, change in the hyoglossus and mylohyoid muscles, recurrence, lymph node metastasis, and complications were evaluated.

Results. Significant differences were found between LRF and FF for signal intensity ($P < .001$) in all 3 periods, with LRF mostly isointense with muscle on T1-weighted images (T1WIs) and FF producing mixed hyperintensity with muscular striations in all cases in T1WIs and T2-weighted images (T2 WIs). Margin definition was similar between groups in the early period, but sharp margins were more common in FF after 4 months ($P \leq .018$). LRF was significantly smaller than FF in all periods ($P \leq .017$). Both mylohyoid and hyoglossus enlargements were common in the early period in both groups, but all cases became atrophic later.

Conclusions. MRI can differentiate LRFs from FFs in a variety of parameters after flap reconstructive surgery for tongue cancer. (Oral Surg Oral Med Oral Pathol Oral Radiol 2021;131:356−363)

The tongue plays crucial roles in mastication, swallowing, speech, and oral hygiene.[1] Carcinoma of the tongue constitutes 40% to 50% of oral cavity cancers, with a high incidence rate.[2-8] Common risk factors for tongue carcinoma include smoking and alcohol abuse.[2,9-13] This lesion has a poorer prognosis compared with other oral cavity carcinomas because of the complexity of lingual anatomy.[13,14] Therefore, patients with tongue cancer may suffer from severe dysphagia and dysarthria after total glossectomy.

The normal anatomy of the tongue is distorted after flap reconstructive surgery. The normal reconstructive flap can be mistaken for recurrence of the neoplasm. In addition, physical examination of postoperative patients is difficult. Thus, it is paramount for radiologists to identify the normal appearance of reconstructive flaps and the altered anatomy of the tongue.[15]

Noninvasive magnetic resonance imaging (MRI) provides excellent soft tissue definition and multidirectional imaging capability. MRI can visualize the components and extent of flaps, recurrence of tumor, lymph node metastasis, and complications of surgery. Previous studies have applied MRI for assessing nasoseptal flaps, muscle flaps, and myocutaneous flaps after reconstructive surgery.[16-19] Postoperative MRI can also assess nasoseptal flaps and free flaps (FFs) in endoscopic skull base reconstruction.[20]

Flap reconstruction, including surgery with locoregional flaps (LRFs) and FFs, is an important way to reduce surgical trauma and improve patients' quality of life. The degree of postoperative dysphagia and dysarthria may be related to the type, volume, components, and location of flaps. However, the postoperative radiologic characteristics of these 2 types of flap reconstruction are still unclear. To our knowledge, MRI studies concerning flap reconstructive surgery for tongue cancer are limited. Thus, we aimed to compare the MRI features of LRF and FF reconstruction of the tongue after surgical treatment for carcinoma as evaluated in 3 different periods. We hypothesized that some imaging features would be significantly different between the 2 types of reconstruction and in different periods.

MATERIALS AND METHODS

Patients

This retrospective study was approved by the institutional review board of our hospital, and informed consent was waived because of the retrospective nature of the investigation. Cases of histopathologically confirmed tongue cancer, diagnosed from August 2012 to January 2018,

Statement of Clinical Relevance

In surgery for tongue cancer, locoregional flaps (LRFs) and free flaps (FFs) aid in the repair of tissue defects. Normal flaps may be misinterpreted as recurrent tumor. Magnetic resonance imaging can differentiate LRFs from FFs with regard to many characteristics and can guide postoperative management.

[a]Department of Radiology, First Affiliated Hospital of Fujian Medical University, Fuzhou, Fujian, China.
[b]Department of Radiology, Zhongshan Hospital Affiliated to Xiamen University, Xiamen, Fujian, China.
Received for publication Feb 17, 2020; returned for revision Jul 17, 2020; accepted for publication Aug 1, 2020.

2212-4403/$-see front matter
https://doi.org/10.1016/j.oooo.2020.08.001

were identified. The inclusion criteria were (1) a histopathologic diagnosis of tongue cancer and (2) primary tongue cancer with initial flap reconstructive surgery. The exclusion criteria were (1) poor-quality MRI scans (including severe susceptibility or motion artifacts) and (2) absence of follow-up MRI scans.

As a result, 115 patients (76 males and 39 females; age 52.3 ± 11.8 years; range 22−82 years) were included in the study. In total, 67 patients were treated with LRFs (10 cases with pectoralis flaps, 37 cases with tongue flaps, and 20 cases with buccal flaps) and 48 cases were treated with FFs (25 cases with radial forearm flaps and 23 cases with anterolateral thigh flaps).

The time intervals between the initial surgery and postoperative MRI examination ranged from 14 days to 48 months. We divided the cases on the basis of the time frame of follow-up MRI into 3 groups: 0 to 4 months, 5 to 12 months, and 13 to 48 months after surgery.

MRI techniques

MRI examinations were performed by using a dedicated head matrix coil on a 3.0 Tesla MRI system (MAGNETOM Verio; Siemens Healthcare, Erlangen, Germany) and a 1.5-Tesla MRI system (Signa Infinity Twinspeed; GE Medical Systems, Boston, MA).

MRI protocols included axial gradient-echo T1-weighted imaging (TR/TE 560 ms/20 ms); axial and coronal turbo spin-echo T2-weighted imaging with fat suppression (TR/TE 4600 ms/89 ms), and gradient-echo contrast-enhanced T1WI (TR/TE = 520 ms/2.5 ms) or turbo spin-echo contrast-enhanced T1WI (TR/TE = 500 ms/10.2 ms) in 3 planes. All sequences were uniform, with a field of view (FOV) of 220 mm × 220 mm and slice thickness of 5 mm with an intersection gap of 1 mm.

In all patients, contrast-enhanced T1-weighted images (T1WIs) were obtained after injection of gadopentetate dimeglumine (Gd; Magnevist, Berlex Imaging, Wayne, NJ) at a dose of 0.1 mmol/kg of weight.

Data processing

Two radiologists (with 30 and 9 years of experience) who were blinded to the surgical procedures evaluated the MRI data individually. The senior radiologist made the final decision when there was disagreement. Signal intensity, margins of the flap, maximal size, contrast enhancement, morphology of the ipsilateral mylohyoid and hyoglossus muscles, tumor recurrence, lymph node metastasis, and complications were evaluated.

The *signal intensity* was classified on T1- and T2-weighted imaging as isointense or mixed hyperintense (hyperintense lesions with strip and flake isointense striations) compared with the muscles of the neck. The *margin of the flap* was characterized as sharp or indistinct. *Maximal size* was measured and selected from 3 planes. *Contrast enhancement* was defined as nonenhancement, mild enhancement, moderate enhancement, or extreme enhancement relative to the nonenhanced appearance of normal muscles in the neck.[21] Enhancement patterns included strip and flake striations and ring-like patterns. The *morphologies of the ipsilateral mylohyoid and hyoglossus muscles* were compared with the contralateral structures and characterized as enlarged or atrophic. Tumor recurrence, lymph node metastasis, combined recurrence and metastasis, and complications (hematoma and/or serous retention) were confirmed on the basis of pathologic and clinical information.

Data analysis

Data for the quantitative parameter of maximal size are presented in Table I as mean ± standard deviation (SD). Comparisons of maximal size values between patients with LRF reconstructive surgery and those with FF reconstructive surgery were made with *t* tests.

Table I. MRI features of flaps for the periods of 0-4, 5-12 and 13-48 months

	0-4 months	*5-12 months*	*13-48 months*
Signal intensity: T1WI			
Isointense	45 (42.9%)	38 (53.5%)	37 (69.8%)
Mixed hyperintense	60 (57.1%)	33 (46.5%)	16 (30.2%)
Signal intensity: T2WI			
Isointense	18 (17.1%)	32 (45.1%)	35 (66.0%)
Mixed hyperintense	87 (82.9%)	39 (54.9%)	18 (34.0%)
Margin			
Sharp	25 (23.8%)	40 (56.3%)	39 (73.6%)
Indistinct	80 (76.2%)	31 (43.7%)	14 (26.4%)
Maximal size (cm)	4.91±1.61	4.02±1.92	3.23±1.62
Contrast enhancement			
Non-enhancement	2 (1.9%)	21 (29.6%)	34 (64.1%)
Mild	44 (41.9%)	42 (59.2%)	17 (32.1%)
Moderate	57 (54.3%)	6 (8.4%)	2 (3.8%)
Extreme	2 (1.9%)	2 (2.8%)	0 (0%)
Ipsilateral mylohyoid			
Enlarged	52 (65.0%)	0 (0)	0 (0)
Atrophic	28 (35.0%)	45 (100%)	42 (100%)
Ipsilateral hyoglossus			
Enlarged	46 (64.8%)	0 (0)	0 (0)
Atrophic	25 (35.2%)	42 (100%)	33 (100%)
Tumor recurrence	0	0	2
Lymph node metastasis	5	3	3
Recurrence and metastasis	1	0	0
Complication			
Hematoma	4	0	0
Serous retention	8	0	0

T1WI, T1-weighted image; T2WI, T2-weighted image.

Comparisons of the categorical variables were made with either Pearson's χ^2 test or Fisher's exact test. Statistical analysis was conducted by using SPSS software version 24.0 (IBM, Armonk, NY). A P value less than .05 was defined as a significant difference.

RESULTS

Table I provides a summary of the MRI features of flaps for the periods 0 to 4 months, 5 to 12 months, and 13 to 48 months. Tables II, III, and IV summarize the MRI features of LRFs and FFs in the 3 different periods 0 to 4 months, 5 to 12 months, and 13 to 48 months. The variations in numbers of cases over the 3 periods represent patients lost to follow-up.

The signal intensities of LRFs and FFs in both T1WIs and T2WIs were significantly different in all 3 periods (all $P < .001$). The majority of LRFs showed isointensity on T1WIs in all 3 periods. Most LRF cases had mixed hyperintense signals at 0 to 4 months and isointense signals in the 5- to 12-month and 13- to 48-month periods postoperatively on T2WIs (Figure 1). However, all FF reconstructions had mixed hyperintense signals in all periods on both T1WIs and T2WIs, which explains the significance of differences between LRFs and FFs. The mixed hyperintensity of FFs on both T1WIs and T2WIs included strip and flake isointense muscular striations (Figure 2). In particular, 18 of the 52 FF cases classified as mixed hyperintensity showed areas of obvious hyperintensity on T2WIs at 0 to 4 months after surgery, and this may be related to ischemia, edema, inflammation, and hemorrhage.

The margins of both LRFs and FFs were mostly indistinct in the period 0 to 4 months after surgery and not significantly different ($P = .097$) as depicted in Figure 1. Both types of flaps tended to have sharper margins in the later periods, but FFs were significantly more likely than LRFs to produce sharp margins ($P \leq .018$). The maximal size of the LRF was significantly smaller than that of the FF in all 3 time frames ($P \leq .017$). Both types of flaps

Table II. MRI features of local-regional flap and free flap reconstruction in the period of 0-4 months

	Locoregional flap	*Free flap*	*Total*	*P*
Signal intensity: T1WI				
Isointense	45	0	45	**<.001**
Mixed hyperintense	8	52	60	
Signal intensity: T2WI				
Isointense	18	0	18	**<.001**
Mixed hyperintense	35	52	87	
Margin				
Sharp	9	16	25	**.097**
Indistinct	44	36	80	
Maximal size (cm)	4.38± 1.84	5.44 ±1.11		**.001**
Contrast enhancement				
Non-enhancement	1	1	2	.410
Mild	19	25	44	
Moderate	31	26	57	
Extreme	2	0	2	
Ipsilateral mylohyoid				
Enlarged	29	23	52	.851
Atrophic	15	13	28	
Ipsilateral hyoglossus				
Enlarged	27	19	46	.587
Atrophic	13	12	25	
Tumor recurrence	0	0	0	
Lymph node metastasis	2	3	5	
Recurrence and metastasis	0	1	1	
Complication				
Hematoma	2	2	4	.679
Serous retention	5	3	8	

P values in bold type: Statistically significant difference.
T1WI, T1-weighted image; T2WI, T2-weighted image.

Table III. MRI features of local-regional flap and free flap reconstruction in the period of 5-12 months

	Locoregional flap	*Free flap*	*Total*	*P*
Signal intensity: T1WI				
Isointense	38	0	38	**<.001**
Mixed hyperintense	6	27	33	
Signal intensity: T2WI				
Isointense	32	0	32	**<.001**
Mixed hyperintense	12	27	39	
Margin				
Sharp	20	20	40	**.018**
Indistinct	24	7	31	
Maximal size (cm)	3.60 ± 2.21	4.71 ± 1.02		**.017**
Contrast enhancement				
Non-enhancement	10	11	21	.362
Mild	28	14	42	
Moderate	4	2	6	
Extreme	2	0	2	
Ipsilateral mylohyoid				
Enlarged	0	0	0	
Atrophic	29	16	45	
Ipsilateral hyoglossus				
Enlarged	0	0	0	
Atrophic	26	16	42	
Tumor recurrence	0	0	0	
Lymph node metastasis	1	2	3	
Recurrence and metastasis	0	0	0	
Complication				
Hematoma	0	0	0	
Serous retention	0	0	0	

P values in bold type: Statistically significant difference.
T1WI, T1-weighted image; T2WI, T2-weighted image.

Table IV. MRI features of local-regional flap and free flap reconstruction in the period of 13-48 months

	Locoregional flap	*Free flap*	*Total*	*P*
Signal intensity: T1WI				
Isointense	37	0	37	**<.001**
Mixed hyperintense	1	15	16	
Signal intensity: T2WI				
Isointense	35	0	35	**<.001**
Mixed hyperintense	3	15	18	
Margin				
Sharp	24	15	39	**.017**
Indistinct	14	0	14	
Maximal size (cm)	2.58 ± 1.34	4.87 ± 0.97		**<.001**
Contrast enhancement				
Non-enhancement	24	10	34	1.0
Mild	12	5	17	
Moderate	2	0	2	
Extreme	0	0	0	
Ipsilateral mylohyoid				
Enlarged	0	0	0	
Atrophic	33	9	42	
Ipsilateral hyoglossus				
Enlarged	0	0	0	
Atrophic	24	9	33	
Tumor recurrence	2	0	2	
Lymph node metastasis	3	0	3	
Recurrence and metastasis	0	0	0	
Complication				
Hematoma	0	0	0	
Serous retention	0	0	0	

P values in bold type: Statistically significant difference.
MRI, magnetic resonance imaging; T1WI, T1-weighted image; T2WI, T2-weighted image.

shrank gradually between the first and second periods (see Figures 1 and 2), but the average size of FF reconstructions did not decrease between the 5- to 12-month and 13- to 48-month periods.

The contrast enhancement of both LRFs (see Figure 1) and FFs (see Figure 2) gradually became less intense over the 3 periods of follow-up ($P \geq .362$). Three cases of LRF showed mild ring-like enhancement at 5 to 12 months (1 case) or at 13 to 48 months (2 cases). All FFs depicted strip and flake striations of contrast enhancement in all 3 time frames. The majority of LRFs and FFs were characterized by enlargement of the ipsilateral mylohyoid and hyoglossus muscles at 0 to 4 months, but there was no significant difference between the types of flap in either muscle ($P \geq .587$). After 4 months, however, all cases of LRF and FF reconstructions were atrophic in both muscles (see Figure 1).

Recurrence of tongue cancer occurred in 2 LRF cases at 13 to 48 months at the inferoposterior interface of the flap and the residual tongue tissue. However, recurrent lingual carcinoma occurred in association with a metastasis to the lymph nodes in 1 FF case in the first period. Lymph node metastasis by itself was more common and occurred in the first 2 periods in both types of flaps and in the 13- to 48-month period in 3 LRF cases. One case of metastasis to the ipsilateral parotid lymph node occurred 3 years after surgery. Hematoma (4 cases characterized by hyperintensity on T1WIs) and serous retention (8 cases) occurred in the first period only (see Figure 2). There was no significant difference in the proportions of hematoma and serous retention between LRFs and FFs ($P = .679$).

DISCUSSION

We demonstrated that some MRI features were significantly different between LRFs and FFs after flap reconstructive surgery for tongue cancer. Most cases reconstructed with LRFs demonstrated isointensity with the neck muscles on T1WIs but mixed hyperintensity on T2WIs at 0 to 4 months after surgery. The main structure in the LRFs is the muscular component. Therefore, postoperative ischemia, edema, inflammation, and hemorrhage might increase the water content in the flap, especially in the period 4 to 6 weeks postoperatively.[22,23] Increased moisture could prolong both the T1 and T2 of flap tissues, which causes the difference in signal intensity on T1WIs and T2WIs. In contrast to LRFs, all FF cases had mixed hyperintense signals in both T1WIs and T2WIs. This may be attributed to the fat composition of the free flap, intermixed with strip and flake isointense muscular striations.

The margins of both LRFs and FFs ranged from sharp or well-defined to indistinct or ill-defined. A significantly greater number of FFs showed sharper margins compared with LRFs after the first 4 months. These results could be explained by the inherent differences in the histology and healing patterns between the 2 types of flaps. LRFs mainly exhibited the intensity of the muscle, mimicking the signal intensity of the tongue muscle, and, therefore, were difficult to identify in the tongue. In contrast, the FF, with its fat composition and mixed signal intensity, could be easily distinguished from adjacent anatomic structures. Moreover, some LRFs showed more ill-defined margins in the later period (13−48 months) as a result of atrophy.

The maximal size of both LRFs and FFs gradually became smaller, which may be attributed to the denervation of muscles. Chronic denervation is characterized by muscular striations, which change the T1WI pattern from isointensity to hyperintensity.[24,25] FFs were significantly larger than LRFs in all 3 periods because FFs were taken from distant sites with adequate muscular tissue, whereas the LRFs were taken from the restricted area around the tongue. In addition, the more muscular component of LRFs led to more significant shrinkage during the follow-up periods compared with that of

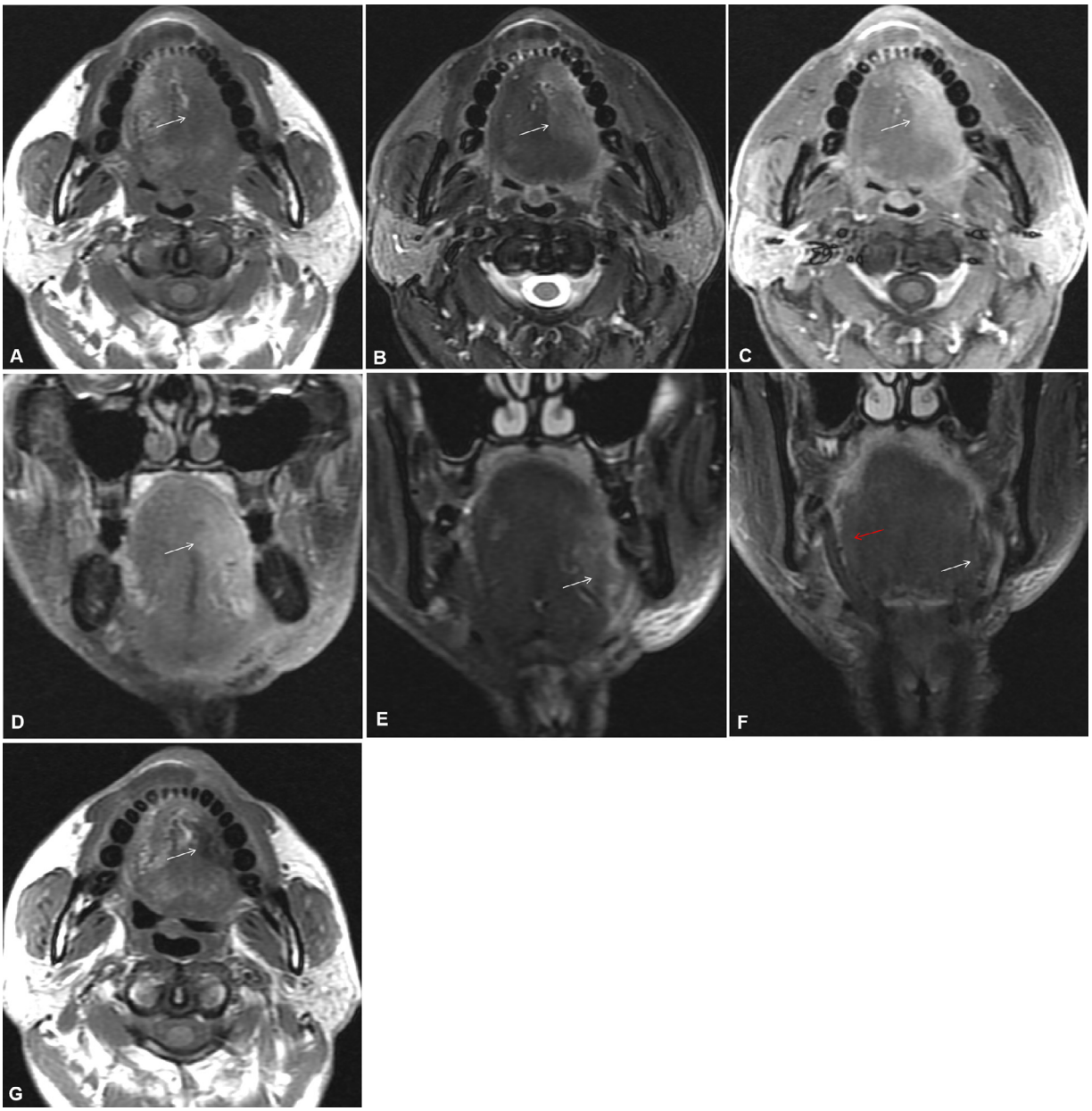

Fig. 1. A 44-year-old man with cancer in the left body of the tongue following locoregional flap reconstruction. Parts A through E were obtained 1 month (in the period 0−4 months) after surgery. The flap shows isointensity with muscle on axial T1-weighted images (T1WIs), as indicated by the white arrow in **(A)** and hyperintensity on axial fast-spin (fs) T2-weighted images (T2WIs), as indicated by the white arrow in **(B)**. Contrast-enhanced axial fast-spin T1-weighted images (T1WIs) **(C)** and coronal fs-T1WIs **(D)** demonstrate moderate enhancement with indistinct borders, as indicated by the white arrows. On coronal fs-T2WIs **(E)**, the enlarged left hyoglossus muscle shows hyperintensity *(white arrow)*. Part F was obtained 7 months (in the period 5−12 months) after surgery. The left mylohyoid muscle shows atrophy *(white arrow)* compared with the normal-appearing right mylohyoid muscle *(red arrow)* on coronal fs-T2WIs. Part G was obtained 28 months (in the period 13−48 months) after surgery. The flap demonstrates isointensity and atrophy *(white arrow)* on axial T1WIs.

FFs, which were substantially unchanged in maximal size. Tarsitano et al. suggested that individual tissue healing processes can also lead to flap shrinkage.[26]

Degrees of contrast enhancement of flaps varied from nonenhancement to extreme enhancement. We found that enhancement of both LRFs and FFs decreased in the follow-up periods. The reduction in enhancement of the flaps was correlated with decreased volume of denervated muscle and enlarged interstitial space.[23,27,28] As previously reported, nonenhancement and delayed enhancement of flaps are the result of vascular dysfunction and fibrous connective tissue

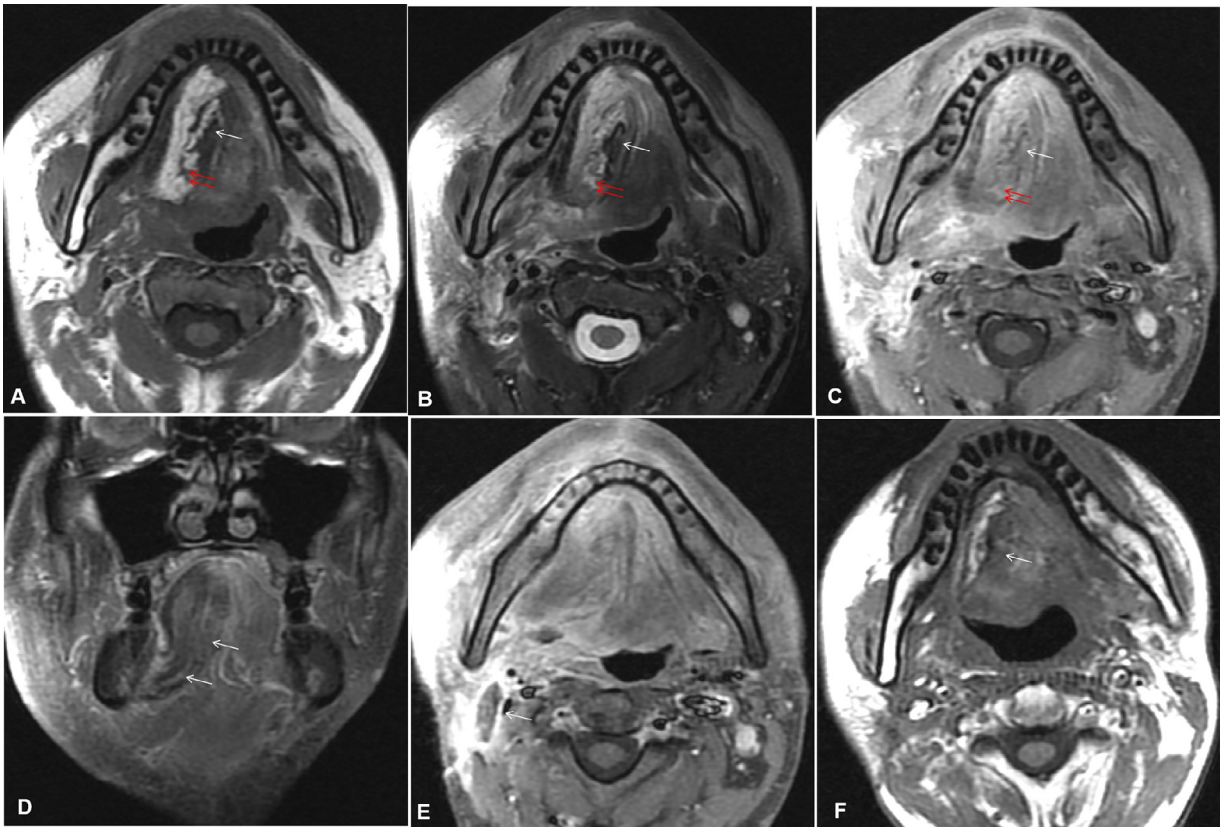

Fig. 2. A 40-year-old man with cancer in the right body of the tongue after free flap reconstruction. Parts A through E were obtained 27 days (in the period 0−4 months) after surgery. The flap shows mixed hyperintensity on axial T1-weighted images (T1WIs) in **(A)** and axial fast-spin (fs) T2-weighted images (T2WIs) **(B)**. Strip and flake muscular striations appear as isointense with muscle on axial T1WIs **(A)**, as indicated by the white and red arrows, The corresponding axial fast-spin (fs) T2WI **(B)** shows isointensity *(white arrow)* with some areas of hyperintensity *(red arrows)*. Subcutaneous effusion is seen in the maxillofacial regions on the right side. Strip and flake muscular striations are seen on axial contrast-enhanced fs-T1WIs **(C)**, as indicated by the white and red arrows and coronal contrast-enhanced fs-T1WIs **(D)**, as indicated by the white arrows. In part E, serous retention displays as a ring-like enhancement at the posterolateral aspect of the right carotid sheath on axial contrast-enhanced fs-T1WIs *(white arrow)*. Part F was obtained 8 months (in the period 5−12 months) after surgery. Axial T1WI **(F)** shows absorption of serous retention and the flap demonstrates mixed hyperintensity and atrophy with reduction of muscular striations *(white arrow)*.

formation.[22,29,30] We also found mild ring-like enhancement of flaps with isointensity to muscle on T2WIs in our study, which might be related to postoperative scar formation and shrinkage.[23]

The ipsilateral mylohyoid and hyoglossus muscles showed enlargement in most cases of both LRFs and FFs as a result of swelling in the 0- to 4-month period (most prominently at 1−1.5 months), but there was no significant difference in the proportion of enlarged and atrophic changes between the 2 types of flaps. All flaps of both types had become shrunken at 5 to 12 months and 13 to 48 months postoperatively. We believe that extrinsic muscle atrophy was a result of denervation because of the damage to the hypoglossal nucleus or hypoglossal nerve during surgery. As a result, the water of damaged muscles shifted from the intracellular space to the extracellular space.[23,27] The variable characteristics of signal intensity on T2WIs might reflect vascular damage, neovascularization, and denervated muscles.

Tongue cancer may recur within weeks to years postoperatively and may display MRI manifestations similar to those of the primary tumor.[30] Previous studies have indicated that the tongue has a rich lymphatic drainage system with abundant interconnectivity.[31] Metastasis of tongue cancer tends to involve level I, II, and III cervical lymph nodes. In one of our cases, ipsilateral parotid lymph node metastasis was found 3 years after surgery. The recurrence of tongue cancer produces moderately high signal intensity on T2WIs without a definite muscular component. Compared with flap tissue, recurrent tumor had greater volume, more indistinct margins, and more obvious enhancement over time. Our study also found that recurrence of tongue cancer was at the inferoposterior interface of the flap

and the residual tongue tissue, which is consistent with previous research.[23]

In patients undergoing flap reconstruction surgery, complications such as hematoma, serous retention, abscess, necrosis, infection, and fistula, should be assessed carefully.[30] They often occur in the early period after surgery. In this study, 4 cases of hematoma in the area of surgery showed hyperintensity on T1WIs, probably because of the lack of methemoglobin.[19] We found serous retention displayed as a ring-like enhancement at 0 to 4 months after surgery. The hematomas and serous retention eventually were resorbed during the follow-up period, and no such complications were detected in the later periods.

There are some potential limitations to our study. First, its retrospective nature may have led to bias in case selection. Thus, a multicenter prospective investigation with a larger sample size is required to confirm the findings of this study and to ensure reproducibility of imaging parameters as predictors of clinical outcomes. Second, because of the short follow-up period, clinical outcomes were not available. Another potential limitation was that advanced MRI techniques, such as diffusion-weighted imaging, were not used in the study.

CONCLUSIONS

This investigation demonstrated that MRI could differentiate LRFs from FFs after reconstructive surgery for tongue cancer. The main manifestations of LRFs indicated the muscle component, resulting in a T1WI signal intensity isointense with muscle in the large majority of cases. In contrast, FFs produced a mixed hyperintensity on both T1WIs and T2WIs in every case. Most surgical margins were indistinct in both flap types in the period 0 to 4 months after surgery but FFs were significantly more likely than LRFs to develop sharply defined borders in the later periods. The maximal size of the LRFs was significantly smaller than that of the FFs at all periods, but whereas LRFs continued to shrink with time, FFs, on average, remained the same size in the last 2 periods. Contrast enhancement of both LRFs and FFs decreased during the follow-up periods.

DISCLOSURE

All procedures performed in the studies involving human participants were in accordance with the ethical standards of the institutional and local Ethical Committee, and with the tenets of the 1964 Helsinki Declaration and its later amendments.

REFERENCES

1. Urken ML, Moscoso JF, Lawson W, Biller HF. A systematic approach to functional reconstruction of the oral cavity following partial and total glossectomy. *Arch Otolaryngol Head Neck Surg*. 1994;120:589-601.
2. La'porte SJ, Juttla JK, Lingam RK. Imaging the floor of the mouth and the sublingual space. *RadioGraphics*. 2011;31:1215-1230.
3. Warnakulasuriya S. Causes of oral cancer—an appraisal of controversies. *Br Dent J*. 2009;207:471-475.
4. Dhanuthai K, Rojanawatsirivej S, Thosaporn W, et al. Oral cancer: a multicenter study. *Med Oral Patol Oral Cir Bucal*. 2018;23:e23-e29.
5. Nithya C, Pandey M, Naik B, et al. Patterns of cervical metastasis from carcinoma of the oral tongue. *World J Surg Oncol*. 2003;1:10.
6. Rubin SJ, Gurary EB, Qureshi MM, et al. Stage II oral tongue cancer: survival impact of adjuvant radiation based on depth of invasion. *Otolaryngol Head Neck Surg*. 2019;160:77-84.
7. Steens SCA, Bekers EM, Weijs WLJ, et al. Evaluation of tongue squamous cell carcinoma resection margins using ex-vivo MR. *Int J CARS*. 2017;12:821-828.
8. Chen WB, Zhang CX, Zhang SX, et al. Application value of MRI combined with positron emission tomography (PET)/CT in diagnosis and preoperative staging of tongue squamous cell carcinoma. *J Med Imag Radiat Oncol*. 2015;59:170-178.
9. Mukherji SK, Pillsbury HR, Castillo M. Imaging squamous cell carcinomas of the upper aerodigestive tract: what clinicians need to know. *Radiology*. 1997;205:629-646.
10. Muraki AS, Mancuso AA, Harnsberger HR, Johnson LP, Meads GB. CT of the oropharynx, tongue base and floor of the mouth: normal anatomy and range of variations and applications in staging carcinoma. *Radiology*. 1983;148:725-731.
11. Li R, Fakhry C, Koch WM, Gourin CG. The Effect of tumor subsite on short−term outcomes and costs of care after oral cancer surgery. *Laryngoscope*. 2013;123:1652-1659.
12. Almangush A, Bello IO, Coletta RD, et al. For early-stage oral tongue cancer, depth of invasion and worst pattern of invasion are the strongest pathological predictors for locoregional recurrence and mortality. *Virchows Arch*. 2015;467:39-46.
13. Mazziotti S, Ascenti G, Scribano E, et al. CT-MR integrated diagnostic imaging of the oral cavity: neoplastic disease. *Radiol med*. 2013;118:123-139.
14. Koo BS, Lim YC, Lee JS, Choi EC. Recurrence and salvage treatment of squamous cell carcinoma of the oral cavity. *Oral Oncol*. 2006;42:789-794.
15. Trotta BM, Pease CS, Rasamny JJ, Raghavan P, Mukherjee S. Oral cavity and oropharyngeal squamous cell cancer: key imaging findings for staging and treatment planning. *RadioGraphics*. 2011;31:339-354.
16. Lall C, Tirkes TA, Patel AA, et al. Flaps, slings, and other things: CT after reconstructive surgery—expected changes and detection of complications. *Am J Roentgenol*. 2012;198:W521-W533.
17. Hudgins PA. Flap reconstruction in the head and neck: expected appearance, complications, and recurrent disease. *Eur J Radiol*. 2002;44:130-138.
18. Tomura N, Watanabe O, Hirano Y, Kato K, Takahashi S, Watarai J. MR imaging of recurrent head and neck tumors following flap reconstructive surgery. *Clin Radiol*. 2002;57:109-113.
19. Stofko DL, Nickles T, Sun H, Dehdashti AR. The value of immediate postoperative MR imaging following endoscopic endonasal pituitary surgery. *Acta Neurochir*. 2014;156:133-140.
20. Learned KO, Adappa ND, Lee JYK, Newman JG, Palmer JN, Loevner LA. MR Imaging evolution of endoscopic cranial defect reconstructions using nasoseptal flaps and their distinction from neoplasm. *AJNR Am J Neuroradiol*. 2014;35:1182-1189.
21. Chong J, Chan LL, Langstein HN, Ginsberg LE. MR imaging of the muscular component of myocutaneous flaps in the head and neck. *AJNR Am J Neuroradiol*. 2001;22:170-174.
22. Varnell RM, Flint PW, Dalley RW, Maravilla KR, Cummings CW, Shuman WP. Myocutaneous flap failure: early detection with Gd-DTPA-enhanced MR imaging. *Radiology*. 1989;173:755-758.

23. Learned KO, Malloy KM, Loevner LA. Myocutaneous flaps and other vascularized grafts in head and neck reconstruction for cancer treatment. *Magn Reson Imaging Clin N Am*. 2012;20:495-513.
24. King AD, Ahuja A, Leung SF, Chan YL, Lam WW, Metreweli C. MR features of the denervated tongue in radiation induced neuropathy. *Br J Radiol*. 1999;72:349-353.
25. Ylä-Kotola TM, Kauhanen MS, Koskinen SK, Asko-Seljavaara SL. Magnetic resonance imaging of microneurovascular free muscle flaps in facial reanimation. *Br J Plast Surg*. 2005;58:22-27.
26. Tarsitano A, Battaglia S, Cipriani R, Marchetti C. Microvascular reconstruction of the tongue using a free anterolateral thigh flap: three-dimensional evaluation of volume loss after radiotherapy. *J Craniomaxillofac Surg*. 2016;44:1287-1291.
27. O'Neill JK, Barrett JA, Cobley T, Devaraj V, Silver DAT. Neurotized free muscle flaps can produce MRI changes mimicking tumour recurrence. *Sarcoma*. 2005;9:133-136.
28. Murakami R, Baba Y, Nishimura R, et al. CT and MR findings of denervated tongue after radical neck dissection. *Am J Neuroradiol*. 1997;18:747-750.
29. Kang MD, Escott E, Thomas AJ, et al. The MR imaging appearance of the vascular pedicle nasoseptal flap. *AJNR Am J Neuroradiol*. 2009;30:781-786.
30. Saito N, Nadgir RN, Nakahira M, et al. Posttreatment CT and MR imaging in head and neck cancer: what the radiologist needs to know. *RadioGraphics*. 2012;32:1261-1282.
31. Fan S, Tang Q-L, Lin Y-J, et al. A review of clinical and histological parameters associated with contralateral neck metastases in oral squamous cell carcinoma. *Int J Oral Sci*. 2011;3:180-191.

Reprint requests:
Dairong Cao, Department of Radiology
First Affiliated Hospital of Fujian Medical University
20 Cha-Zhong Road
Fuzhou
Fujian 350005
P.R. China.
Dairongcao@163.com